Trajectory Tracking of a 3DOF Laboratory Helicopter Under Input and State Constraints

authored by **T. Kiefer, K. Graichen, and A. Kugi**

and published in *IEEE Transactions on Control Systems Technology*.

Cite this article as:

T. Kiefer, K. Graichen, and A. Kugi, "Trajectory tracking of a 3dof laboratory helicopter under input and state constraints", *IEEE Transactions on Control Systems Technology*, vol. 18, pp. 944–952, 2010. DOI: 10.1109/TCST.2009.2028877

BibTex entry:

```
@article{Kiefer10,
  author = {Kiefer, T. and Graichen, K. and Kugi, A.},
  title = {Trajectory Tracking of a 3DOF Laboratory Helicopter Under Input and State Constraints},
  journal = {IEEE Transactions on Control Systems Technology},
  year = {2010},
  volume = {18},
  pages = {944--952},
  doi = {10.1109/TCST.2009.2028877}
}
```

Link to original paper:

http://dx.doi.org/10.1109/TCST.2009.2028877

Contact:

Automation and Control Institute (ACIN)
Vienna University of Technology
Gusshausstrasse 27-29/E376
1040 Vienna, Austria

Internet: www.acin.tuwien.ac.at
E-mail: office@acin.tuwien.ac.at
Phone: +43 1 58801 37601
Fax: +43 1 58801 37699

Trajectory tracking of a 3DOF laboratory helicopter under input and state constraints

Thomas Kiefer, Knut Graichen, and Andreas Kugi, *Member, IEEE,*

Abstract

This paper deals with the tracking control design of a helicopter laboratory experimental set–up. In order to be able to realize highly dynamic flight maneuvers both input and state constraints have to be systematically accounted for within the control design procedure. The mathematical model being considered constitutes a nonlinear mathematical mechanical system with two control inputs and three degrees–of–freedom. The control concept consists of an inversion–based feedforward controller for trajectory tracking and a feedback controller for the trajectory error dynamics. The design of the feedforward controller for a setpoint to setpoint flight maneuver is traced back to the solution of a 2–point boundary value problem in the Byrnes–Isidori normal form of the mathematical model. By utilizing special saturation functions the given constraints in the inputs and states can be systematically incorporated in the overall design process. In order to capture model uncertainties and external disturbance an optimal state feedback controller is designed on the basis of the model linearization along the desired trajectories. The proposed control scheme is implemented in a real–time environment and by means of experimental results the feasibility and the excellent performance is demonstrated.

Index Terms

laboratory helicopter, nonlinear control, feedforward control, input constraints, state constraints, boundary value problem.

I. Introduction

The 3DOF helicopter under consideration is a laboratory experiment which is often used in control research and education for the design and implementation of (non-)linear control concepts, see also [1], [2]. As depicted in Fig. 1, the helicopter basically consists of three hinge–mounted rigid body systems. The helicopter base, which can turn about the travel angle q_1, carries the arm which can rotate about the elevation angle q_2. One end of the arm is attached to a counterweight that tares the weight of the third mechanical subsystem, i.e. the helicopter body. The rotation of this body is described by the pitch angle q_3. Two propellers driven by dc–motors are attached to each end of the body. The voltages u_f and u_b supplied to the dc–motors serve as control inputs to the system. They generate the thrusts f_f and f_b acting on the helicopter body. Since only two control inputs are available for controlling 3 degrees–of–freedom, the helicopter represents an underactuated mechanical system. This makes the controller design more challenging compared to the fully actuated case where the number of degrees–of–freedom equals the number of control inputs. Starting with the presentation of the nonlinear mathematical model of the helicopter, the main task of this contribution is the trajectory planning and the tracking control design of the helicopter. Special emphasis is laid on an approach to systematically account for the input constraints in the voltages u_f and u_b of the dc–motors and the state constraint in the pitch angle q_3.

T. Kiefer is with the Rolling Mill Technology department of the AG der Dillinger Hüttenwerke, 66763 Dillingen, Germany (email: thomas.kiefer@dillinger.biz).

K. Graichen, and A. Kugi are with the Automation and Control Institute, Vienna University of Techology, Gußhausstr. 27-29, 1040 Vienna, Austria (email:{graichen,kugi}@acin.tuwien.ac.at, internet: http://cds.acin.tuwien.ac.at).

Pre-print version of the article: T. Kiefer, K. Graichen, and A. Kugi, "Trajectory tracking of a 3dof laboratory helicopter under input and state constraints", *IEEE Transactions on Control Systems Technology*, vol. 18, pp. 944–952, 2010. DOI: 10.1109/TCST.2009.2028877
The content of this pre-print version is identical to the published paper but without the publisher's final layout or copy editing.

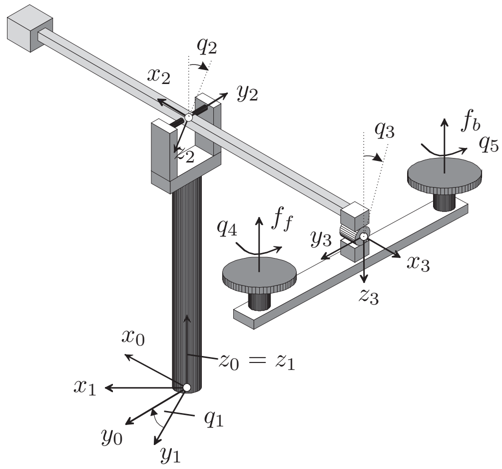

Fig. 1. Schematics of the laboratory experiment 3DOF helicopter.

Some works dealing with the modeling and control of the 3DOF helicopter can already be found in the literature. For example, [3] is devoted to the derivation of a mathematical model of the helicopter but no control strategy is presented therein. By contrast, the authors of [4] focus on a neural–network based adaptive feedback control without going into detail with the mathematical structure of the helicopter. Although the experimental results in [4] are quite satisfactory, the main drawback of this work results from the fact that the (SISO–) controller is developed only for the pitch angle q_3, the essential motion in the travel and elevation axes q_1 and q_2 is neglected. Furthermore, an adaptive identification of the model parameters is topic of [5] which are used in [6] to design adaptive PID–controllers for the overall motion of the helicopter. The results of the controller design are validated by means of experimental data of a 360deg–rotation of the helicopter about the travel axis in about $T = 15\,\mathrm{s}$.

In this contribution, a mathematical model of the helicopter is derived by means of Lagrange's formalism. Based on the approach presented in [7], the very extensive model is simplified for the purpose of controller design. This simplified model still captures the essential nonlinearities of the helicopter system in an accurate way.

Furthermore, the simplified model turns out to be differentially flat [8], [9]. This system property is advantageously utilized in [7] for the design of a flatness–based tracking controller. The controller aims at steering the helicopter along desired trajectories for the flat outputs. The flatness–based control concept achieves accurate tracking but does not directly account for the above mentioned input and state constraints. For instance, a desired trajectory for the rotation about the travel axis q_1 must be sufficiently slow in order to comply with the constraints. Thus, the goal of this contribution is to systematically incorporate input and state constraints into the controller design to be able to perform the desired motion in a more aggressive manner.

The control concept presented in this work relies on a two degrees–of–freedom control structure consisting of an inversion–based feedforward controller and a feedback controller for stabilizing the trajectory error system. The procedure is an extension of the one presented in [10] to time–varying input constraints. The design of the inversion–based feedforward controller is formulated as a two–point boundary value problem (BVP) in the Byrnes–Isidori normal form of the system under consideration, see [11]. Moreover, this approach allows for the systematic incorporation of input constraints [12] and output constraints [13], [14]. By choosing the outputs of the helicopter model as dedicated state variables, the state constraints can be interpreted as output constraints such that the feedforward control design as presented in [14] can directly be applied. In order to

Pre-print version of the article: T. Kiefer, K. Graichen, and A. Kugi, "Trajectory tracking of a 3dof laboratory helicopter under input and state constraints", *IEEE Transactions on Control Systems Technology*, vol. 18, pp. 944–952, 2010. DOI: 10.1109/TCST.2009.2028877
The content of this pre-print version is identical to the published paper but without the publisher's final layout or copy editing.

reject disturbances and account for model uncertainties, an additional feedback controller has to be developed. Here, a time–variant LQ–controller based on the linearization of the system along the desired trajectories will be used.

The paper is organized as follows: the model of the helicopter as well as a detailed formulation of the control task under consideration is given in Section II. The main section, Section III, is devoted to the design of a feedforward controller, starting from the unconstrained case and successively introducing the constraints on both the inputs u_f and u_b and the pitch angle q_3. At the end of this section, a time–variant LQ–feedback controller is designed to stabilize the trajectory error system. The feasibility of the proposed control approach is demonstrated by means of experimental results in Section IV. Finally, the paper closes with a short conclusion in Section V.

II. Problem formulation

The mathematical model of the helicopter laboratory experimental set–up can be derived by means of Lagrange's formalism. The equations of motion can be written in matrix notation in the well–known form

$$D(q)\ddot{q} + C(q,\dot{q})\dot{q} + g(q) = Q, \tag{1}$$

with the generalized inertia matrix $D(q)$, the Coriolis matrix $C(q,\dot{q})$, the gravity vector $g(q)$ and the generalized forces Q, see, e.g., [15], [16].

A detailed derivation of the helicopter model can be found in [7]. Therein, the rotation of the propellers, described by the angles q_4 and q_5 according to Fig. 1, and the dynamics of the dc–motors are taken into account in addition to the three degrees–of–freedom given by the travel, elevation, and pitch angle q_1, q_2 and q_3. For the controller design, the model has to be simplified such that it can be handled within the framework of nonlinear control theory. However, this simplified model should still capture the essential nonlinearities of the system. In this context, the fast dynamics of the electrical subsystems given by the dc–motors and the dynamics of the propellers, described by the angles q_4 and q_5, can be approximated in a quasi–static way utilizing the singular perturbation theory, see, e.g., [17]. As a consequence, the model can be very well described by only three degrees–of–freedom, namely q_1, q_2 and q_3, with the voltages u_f and u_b as the control inputs of the system. Neglecting the rotor dynamics of the propellers results in a static relation between the thrusts f_f and f_b and the voltages u_f and u_b applied to the dc–motors. It can be shown that this relation constitutes a quadratic characteristics of the form, see, e.g., [18]

$$f_i = \begin{cases} k_+ u_i^2, \ u_i \geq 0 \\ k_- u_i^2, \ u_i < 0 \end{cases}, \ i \in \{f, b\}. \tag{2}$$

The coefficients k_+ and k_- of (2) are identified by measurements, cf. Fig. 2. The numerical values are given in Table I.

In a second step, the complexity of the model structure can be further reduced by neglecting terms with small influence on the overall kinetic energy. This procedure guarantees that the Lagrangian structure of the system is preserved. In this way, the kinetic energy is simplified such that the generalized inertia matrix $D(q)$ reduces to a diagonal matrix with constant entries d_{jj}, $j = 1, 2, 3$, i.e. $D(q) = \mathrm{diag}(d_{11}, d_{22}, d_{33})$ with the consequence $C(q,\dot{q}) = 0$ in (1), see [7] for more details.

For small angles of the elevation axis q_2, it is further possible to neglect certain expressions in the external forces on the right hand side of (1). The latter simplification can also be interpreted in a geometrical way, namely it is assumed that the rotors always lie in a plane parallel to the z_1-axis, see [7]. Then, the equations

Pre-print version of the article: T. Kiefer, K. Graichen, and A. Kugi, "Trajectory tracking of a 3dof laboratory helicopter under input and state constraints", *IEEE Transactions on Control Systems Technology*, vol. 18, pp. 944–952, 2010. DOI: 10.1109/TCST.2009.2028877
The content of this pre-print version is identical to the published paper but without the publisher's final layout or copy editing.

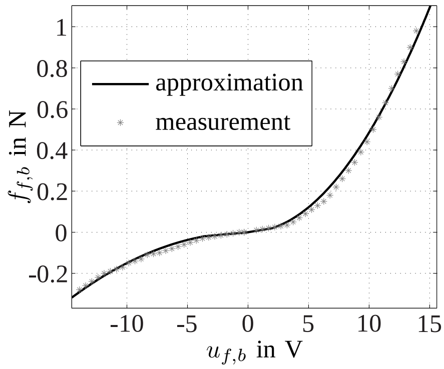

Fig. 2. Measured and identified characteristics of the thrusts as a function of the motor voltages.

of motion read as

$$\ddot{q}_1 = b_1 \cos(q_2) \sin(q_3) v_1 \tag{3a}$$

$$\ddot{q}_2 = a_1 \sin(q_2) + a_2 \cos(q_2) + b_2 \cos(q_3) v_1 \tag{3b}$$

$$\ddot{q}_3 = a_3 \cos(q_2) \sin(q_3) + b_3 v_2 \tag{3c}$$

with the sum and the difference v_1 and v_2 of the front and back thrusts f_f and f_b

$$v_1 = f_f + f_b \tag{4a}$$

$$v_2 = f_f - f_b \tag{4b}$$

as the new control inputs and the coefficients $a_j, b_j, j = 1, 2, 3$ depending on the masses and the geometric parameters. The numerical values of the coefficients are given in Table I. Based on the mathematical model (3),

k_+	$4.855e^{-3} \frac{\mathrm{N}}{\mathrm{V}^2}$	k_-	$-1.503e^{-3} \frac{\mathrm{N}}{\mathrm{V}^2}$
a_1	$-1.1713 \frac{\mathrm{rad}}{\mathrm{s}^2}$	b_1	$-0.6354 \frac{\mathrm{rad}}{\mathrm{kgm}}$
a_2	$0.3946 \frac{\mathrm{rad}}{\mathrm{s}^2}$	b_2	$-0.6523 \frac{\mathrm{rad}}{\mathrm{kgm}}$
a_3	$-0.5326 \frac{\mathrm{rad}}{\mathrm{s}^2}$	b_3	$4.6276 \frac{\mathrm{rad}}{\mathrm{kgm}}$

TABLE I
PARAMETERS OF THE MATHEMATICAL MODEL.

a transition of the 3DOF helicopter between stationary setpoints $\left(q_{1,0}^*, q_{2,0}^*, q_{3,0}^*\right) \rightarrow \left(q_{1,T}^*, q_{2,T}^*, q_{3,T}^*\right)$ within the finite time interval $t \in [0, T]$ is formulated as a two–point boundary value problem (BVP). The trajectory of such a flight maneuver has to satisfy the following boundary conditions (BCs)

$$q_1(0) = q_{1,0}^*, \qquad q_1(T) = q_{1,T}^*, \qquad \dot{q}_1|_{0,T} = 0, \tag{5a}$$

$$q_2(0) = q_{2,0}^*, \qquad q_2(T) = q_{2,T}^*, \qquad \dot{q}_2|_{0,T} = 0, \tag{5b}$$

$$q_3(0) = q_{3,0}^* = 0, \qquad q_3(T) = q_{3,T}^* = 0, \qquad \dot{q}_3|_{0,T} = 0 \tag{5c}$$

due to the steady state conditions of the starting and the terminal point at $t \in \{0, T\}$. The design of the feedforward controller has to account for the input constraints

$$u_{f,b} \in [u^-, u^+] \tag{6}$$

and for given constraints in the pitch angle

$$q_3 \in [q_3^-, q_3^+]. \tag{7}$$

Pre-print version of the article: T. Kiefer, K. Graichen, and A. Kugi, "Trajectory tracking of a 3dof laboratory helicopter under input and state constraints", *IEEE Transactions on Control Systems Technology*, vol. 18, pp. 944–952, 2010. DOI: 10.1109/TCST.2009.2028877
The content of this pre-print version is identical to the published paper but without the publisher's final layout or copy editing.

Henceforth, a 360deg–rotation of the helicopter about the travel axis in $T = 10\,\mathrm{s}$ will be considered for demonstration purposes, i.e.

$$q^*_{1,0} = q^*_{2,0} = q^*_{2,T} = 0 \quad \text{and} \quad q^*_{1,T} = 2\pi. \tag{8}$$

Furthermore, the constraints according to (6) and (7) are specified by the limits

$$u^- = 1\mathrm{V}\ ,\ u^+ = 11\mathrm{V} \quad \text{and} \quad q_3^\pm = \pm 50\,\mathrm{deg}. \tag{9}$$

Note that in contrast to the constraints on the input voltages, there is no specific physical reason for the choice of $q_3^\pm = \pm 50\,\mathrm{deg}$ for the state constraints in the pitch angle q_3. This is just used to demonstrate the design method for the trajectory planning with state constraints. In principle all values of $q_3^\pm$ between $\pm 10\,\mathrm{deg}$ and $\pm 80\,\mathrm{deg}$ would be possible. Furthermore, the boundaries for the control inputs in (9) are chosen in such a way that they are close to the physical limits of[1] $u^- = 1\,\mathrm{V}$ and $u^+ = 11\,\mathrm{V}$. Consequently there are still some reserves for the contribution of the feedback controller.

III. Controller design with constraints

In order to systematically account for the constraints within the controller design for the helicopter, we will henceforth benefit from the method presented in [10]. Thereby, the design of the tracking controller is based on the two degrees–of–freedom control scheme as depicted in Fig. 3. On the assumption of an exact mathematical model of the plant Σ and that no disturbances are acting on the system, the feedforward controller Σ^{FF} is designed to ensure an exact tracking of the reference trajectory y^*. In order to stabilize the trajectory error system and to account for model uncertainties and disturbances a feedback controller Σ^{FB} is used. The reference trajectory generator Σ^* provides a sufficiently smooth reference trajectory $y^*(t)$ for both the feedback and the feedforward controller.

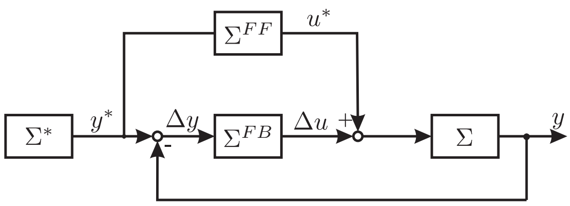

Fig. 3. Structure of the two degrees–of–freedom control scheme with system Σ, feedback controller Σ^{FB}, feedforward controller Σ^{FF}, and reference trajectory generator Σ^*.

The main part of this section is concerned with the design of the feedforward controller Σ^{FF} and the reference trajectory generator Σ^* in consideration of input and state constraints. From a mathematical point of view the 12 BCs (5) together with the 3 second–order ODEs (3) form a two–point boundary value problem for the states q_1, $\dot q_1$, q_2, $\dot q_2$, q_3, $\dot q_3$ depending on the inputs v_1 and v_2 (resp. u_f and u_b). In order to find a solution of this BVP, the so–called inversion–based feedforward control in the coordinates of the Byrnes–Isidori normal form, see, e.g., [11], [19], [20], will be used.

A. Byrnes–Isidori normal form of the helicopter

Before applying the control design procedure according to [13] to the helicopter model (3), the system has to be transformed to Byrnes–Isidori normal form. For this an appropriate output $y = \{y_1, y_2\}$ has to be defined. Although the choice of this output is in general free, one output is chosen as the pitch angle, i.e. $y_2 = q_3$, in

[1] The propellers are not designed to produce considerable thrusts when applying negative voltages, cf. Fig 2.

Pre-print version of the article: T. Kiefer, K. Graichen, and A. Kugi, "Trajectory tracking of a 3dof laboratory helicopter under input and state constraints", *IEEE Transactions on Control Systems Technology*, vol. 18, pp. 944–952, 2010. doi: 10.1109/TCST.2009.2028877
The content of this pre-print version is identical to the published paper but without the publisher's final layout or copy editing.

order to be able to interpret the state constraint (9) as an output constraint. The only restriction for the remaining output y_1 is that it must be independent of y_2. It turns out that $y_1 = q_2$ is a reasonable choice leading to simple expressions for the system inversion. The relative degree of (3) with respect to the output

$$y = \{q_2, q_3\} \tag{10}$$

calculates to $\{2, 2\}$. Thus, by choosing $\eta = q_1$ for describing the internal dynamics, the system (3) in Byrnes–Isidori normal form follows as

$$\begin{aligned} \ddot{y}_1 &= a_1 \sin(y_1) + a_2 \cos(y_1) + b_2 \cos(y_2) v_1 && \text{(11a)} \\ \ddot{y}_2 &= a_3 \cos(y_1) \sin(y_2) + b_3 v_2 && \text{(11b)} \\ \ddot{\eta} &= b_1 \sin(y_2) \cos(y_1) v_1 . && \text{(11c)} \end{aligned}$$

The BCs (5) and (8) for the reference trajectory formulated in the coordinates y_1, y_2 and η take the form

$$\begin{aligned} &\eta(0) = \eta_0^* = q_{1,0}^*, && \eta(T) = \eta_T^* = q_{1,T}^*, && \dot{\eta}|_{0,T} = 0, && \text{(12a)} \\ &y_1(0) = y_{1,0}^* = q_{2,0}^*, && y_1(T) = y_{1,T}^* = q_{2,T}^*, && \dot{y}_1|_{0,T} = 0, && \text{(12b)} \\ &y_2(0) = y_{2,0}^* = 0, && y_2(T) = y_{2,T}^* = 0, && \dot{y}_2|_{0,T} = 0. && \text{(12c)} \end{aligned}$$

B. Feedforward controller without constraints

In a first step, let us consider the solution of the BVP (11) and (12) when neglecting the constraints (6) and (7). The inversion–based design of the feedforward controller is based on the inverse input–output dynamics [20]. Clearly, in view of (11a) and (11b), the feedforward controller[2]

$$\begin{aligned} v_1^* &= \frac{\ddot{y}_1^* - a_1 \sin(y_1^*) - a_2 \cos(y_1^*)}{b_2 \cos(y_2^*)} && \text{(13a)} \\ v_2^* &= \frac{\ddot{y}_2^* - a_3 \cos(y_1^*) \sin(y_2^*)}{b_3} && \text{(13b)} \end{aligned}$$

can be algebraically determined for the desired output trajectories $y_1^*(t) \in \mathcal{C}^3$ and $y_2^*(t) \in \mathcal{C}^3$. Note that the feedforward controller (13) is independent of the state η^* of the internal dynamics representing the travel axis of the helicopter. Nevertheless, in order to ensure that the BCs (12a) are satisfied by the trajectory $\eta^*(t)$, the BVP of the internal dynamics (11c), (12a) is rewritten by inserting (13a) into (11c)

$$\begin{aligned} \ddot{\eta}^* &= \frac{b_1}{b_2} \tan(y_2^*) \big(\ddot{y}_1^* - a_1 \sin(y_1^*) - a_2 \cos(y_1^*)\big) \cos(y_1^*) \\ &= \bar{\beta}(y_1^*, \ddot{y}_1^*, y_2^*) && \text{(14a)} \\ \eta^*(0) &= q_{1,0}^*, \quad \eta^*(T) = q_{1,T}^*, \quad \dot{\eta}^*|_{0,T} = 0 && \text{(14b)} \end{aligned}$$

with the desired output trajectories $y_1^*(t)$ and $y_2^*(t)$ serving as the input to (14a). Obviously, the BVP (14a) is overdetermined since 4 BCs (14b) have to be satisfied for one second–order ODE (14a). Following the basic idea of the approach presented in [11], the solvability of the BVP requires 2 free parameters $p = (p_1, p_2)$ in the desired output trajectories $y_1^*(t)$ and $y_2^*(t)$. Thereby, some freedom exists concerning how the free parameters are distributed to the two output functions. From a physical point of view, the acceleration $\ddot{\eta}^* = \ddot{q}_1^*$ of the travel axis is directly related to the pitch angle $y_2^* = q_3^*$ of the helicopter body, see Fig. 1. Thus, it is reasonable to provide both parameters p in the second output $y_2^*(t) = \Upsilon_2(t, p)$, whereas the first output is determined as a predefined setup function $y_1^*(t) = \Upsilon_1(t)$.

[2]Henceforth, the index $*$ of a quantity always refers to the corresponding desired trajectories.

Pre-print version of the article: T. Kiefer, K. Graichen, and A. Kugi, “Trajectory tracking of a 3dof laboratory helicopter under input and state constraints”, *IEEE Transactions on Control Systems Technology*, vol. 18, pp. 944–952, 2010. DOI: 10.1109/TCST.2009.2028877
The content of this pre-print version is identical to the published paper but without the publisher’s final layout or copy editing.

The setup functions $\Upsilon_1(t)$ and $\Upsilon_2(t,p)$ are constructed as polynomials, see, e.g. [21], and have to satisfy the BCs (12b) and (12c). The solution of the resulting BVP with free parameters comprises the parameter set p as well as the trajectory $\eta^*(t)$ of the travel axis of the helicopter. Thereby, the parameter set p determines the shape of the output trajectory $y_2^*(t)$.

The solution of this type of BVP with free parameters is a standard task in numerics. Here, the MATLAB function bvp4c is used where a linear interpolation between the corresponding BCs on a uniform mesh with 50 grid points $t_k \in [0,T]$, $k = 1,\ldots,50$, serves as an initial guess for the trajectory $\eta^*(t_k)$. The initial values for the unknown parameters p are set to zero. The robustness and convergence of the numerical solution are enhanced by providing the analytical Jacobian matrix of the ODEs (14).

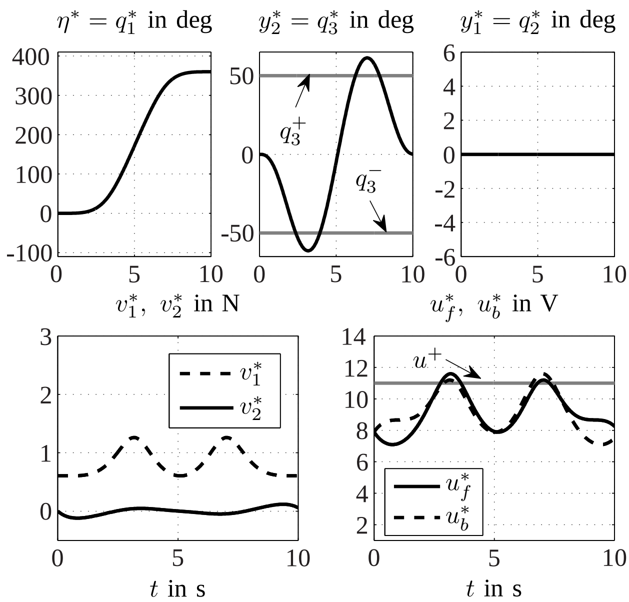

Fig. 4. Results of the feedforward control design without constraints.

The results are presented in Fig. 4 where the upper three pictures show the nominal trajectories η^*, y_1^* and y_2^* for the rotation of the helicopter about the travel–axis by 360deg within a transition time of $T = 10$s. The trajectory $\eta^*(t) = q_1^*(t)$ is strictly monotonically increasing and constitutes a smooth motion of the helicopter. While the elevation angle $y_1^*(t) = q_2^*(t) = 0$ remains in the same position, the under– and over–shoots in the output $y_2^* = q_3^*$ are required to accelerate and decelerate the helicopter about the travel axis. Clearly, the trajectory y_2^* of the pitch angle violates the required constraints given by (7).

The pictures in the lower part of Fig. 4 show the corresponding control inputs v_1^* and v_2^* and the resulting voltages u_f and u_b due to (2). It can be seen that both voltages u_f^* and u_b^* exceed the upper constraint u^+ according to (6).

However, this approach does not yet allow to incorporate the input and state constraints (6) and (7) in a systematic way. The only possibility so far is to change the transition time T and subsequently check whether the constraints are fulfilled or not.

C. *Reformulation of the constrained problem*

In this subsection, the procedure presented in Subsection III-B is extended in such a way that the constraints in the real control inputs according to (6) and the constraint in the pitch angle (7) are systematically taken into account within the feedforward control design.

Pre-print version of the article: T. Kiefer, K. Graichen, and A. Kugi, “Trajectory tracking of a 3dof laboratory helicopter under input and state constraints”, *IEEE Transactions on Control Systems Technology*, vol. 18, pp. 944–952, 2010. DOI: 10.1109/TCST.2009.2028877
The content of this pre-print version is identical to the published paper but without the publisher’s final layout or copy editing.

In contrast to the considerations in [10], where constant input constraints are taken into account for the transformed (virtual) control inputs v_1 and v_2 as they appear in the input–output representation (11), the input constraints (6) in this paper are formulated in the (real) control inputs, namely the voltages u_f and u_b or the thrusts f_f and f_b, respectively. As a result, the constraints of the virtual control inputs v_1 and v_2 become time-varying.

In the following, we will extend the results derived in [10] to explicitly tackle this more general case. Since it is preferable to maintain the decoupled structure of the input–output representation (11) with respect to the inputs v_1 and v_2, the real input constraints (6) are formulated as constraints for the transformed inputs v_1 and v_2 due to (4). An illustration of this transformation of the input constraints is depicted in Fig. 5. Obviously, the constraints in the transformed inputs v_1 and v_2 are no longer constant.

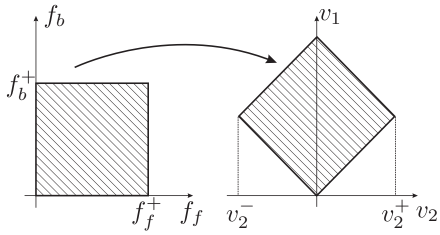

Fig. 5. Transformation of the input constraints.

By combining (2), (4) and (6) with

$$f_i^- = \begin{cases} k_+ \left(u_i^-\right)^2, & u_i \geq 0 \\ k_- \left(u_i^-\right)^2, & u_i < 0 \end{cases}, \quad i \in \{f, b\} \tag{15}$$

and

$$f_i^+ = \begin{cases} k_+ \left(u_i^+\right)^2, & u_i \geq 0 \\ k_- \left(u_i^+\right)^2, & u_i < 0 \end{cases}, \quad i \in \{f, b\} \tag{16}$$

the transformed inputs v_1 and v_2 have to meet the inequality conditions

$$\begin{aligned} 2f_f^- &< v_1 + v_2 < 2f_f^+ \\ 2f_b^- &< v_1 - v_2 < 2f_b^+ . \end{aligned} \tag{17}$$

It is easy to see that (17) is equivalent to

$$\underbrace{f_f^- - f_b^+}_{v_2^-} < v_2 < \underbrace{f_f^+ - f_b^-}_{v_2^+} . \tag{18}$$

and

$$v_1^- \left(v_2\right) < v_1 < v_1^+ \left(v_2\right) \tag{19}$$

with

$$v_1^- \left(v_2\right) = \max\left[\left(2f_f^- - v_2\right), \left(2f_b^- + v_2\right)\right] \tag{20a}$$

$$v_1^+ \left(v_2\right) = \min\left[\left(2f_f^+ - v_2\right), \left(2f_b^+ + v_2\right)\right] . \tag{20b}$$

In this formulation, v_2 has fixed bounds[3], whereas $v_1^\pm$ depend on v_2 as illustrated in Fig. 5. This procedure entails some advantages in the further design steps as will be discussed subsequently.

[3]An equivalent representation can be found by choosing fixed bounds for v_1 with $v_1^- = f_f^- + f_b^-$ and $v_1^+ = f_f^+ + f_b^+$ and varying bounds $v_2^\pm \left(v_1\right)$.

Pre-print version of the article: T. Kiefer, K. Graichen, and A. Kugi, "Trajectory tracking of a 3dof laboratory helicopter under input and state constraints", *IEEE Transactions on Control Systems Technology*, vol. 18, pp. 944–952, 2010. DOI: 10.1109/TCST.2009.2028877
The content of this pre-print version is identical to the published paper but without the publisher's final layout or copy editing.

Although at first glance it seems more meaningful to formulate the problem in the real inputs u_f and u_b, the approach presented in this work is based on the transformed control inputs v_1 and v_2 mainly for two reasons. Firstly, the decoupled structure of the mathematical model (3) or (11), respectively, enables a very compact formulation of the inversion–based feedforward controller, cf. (13). Secondly, the resulting BVP can be solved in a straightforward manner also for time–variant bounds of the input constraints.

In order to directly incorporate the input constraints (18), (19) into the design procedure, let us take advantage of the fact that the feedforward control inputs $v_1^*(t)$ and $v_2^*(t)$ from (13) are directly influenced by the highest time derivatives $\ddot{y}_1^*(t)$ and $\ddot{y}_2^*(t)$ of the desired outputs. As it is suggested in [13], [14], the relations (11a) and (11b) can be used to reformulate the input constraints (18) and (19) with respect to $\ddot{y}_1(t)$ and $\ddot{y}_2(t)$, i.e.

$$\ddot{y}_1^- \leq \ddot{y}_1 \leq \ddot{y}_1^+ \tag{21a}$$

$$\ddot{y}_2^- \leq \ddot{y}_2 \leq \ddot{y}_2^+, \tag{21b}$$

where

$$\begin{aligned} \ddot{y}_1^\pm &= a_1 \sin(y_1^*) + a_2 \cos(y_1^*) + b_2 \cos(y_2^*) v_1^\pm(v_2) \\ &= \alpha_1(y_1^*, y_2^*, v_1^\pm(v_2)) \end{aligned} \tag{22}$$

and

$$\ddot{y}_2^\pm = a_3 \cos(y_1^*) \sin(y_2^*) + b_3 v_2^\pm = \alpha_2(y_1^*, y_2^*, v_2^\pm). \tag{23}$$

hold. Note that the limits $\ddot{y}_1^\pm$ and $\ddot{y}_2^\pm$ are not constant but depend on the outputs y_1^* and y_2^*.

In addition it can be stated that the constraints in the pitch angle $y_2 = q_3$ according to (7), i.e.

$$y_2^* \in [q_3^-, q_3^+], \tag{24}$$

yield constraints directly in the output y_2. As a consequence of (21) and (24), both the input constraints as well as the constraints in the pitch angle can be interpreted as constraints in the outputs and their higher derivatives. This fact is used in Section III-D to reformulate a new BVP which systematically takes into account these constraints.

Remark 1: Note that the consideration of the input constraints (18) and (19) is rather simple for the helicopter model (11) because the input–output dynamics (11a) and (11b) are decoupled with respect to the inputs, i.e. $\ddot{y}_1$ and $\ddot{y}_2$ are affected separately by v_1 and v_2. The general case of feedforward control design under input constraints for general nonlinear MIMO systems is addressed in [13], [21].

D. Incorporation of constraints in the BVP formulation

In [13], [14], the feedforward control design is extended to account for constraints in the outputs and their time derivatives as they are given by (21) and (24). Thereby, the constrained output is represented by means of a saturation function with a new state variable. By successively differentiating this output and introducing new saturation functions in each step, it is possible to derive a new dynamical system which considers the constraints in the output and in its derivatives. The original dynamical system for the unconstrained output is then replaced by this new dynamical system.

In a first step, the more general case with saturations in y_2 and $\ddot{y}_2$ (i.e. in v_2) is treated in more detail, the consideration of the saturation only in $\ddot{y}_1$ (i.e. in v_1) follows as a special case. The output constraint (24) is considered by introducing the smooth saturation function

$$y_2^* = \psi_1\left(\xi_1, \psi_1^\pm\right) \tag{25}$$

which depends on the new state variable $\xi_1(t)$ and the respective saturation limits

$$\psi_1^\pm = q_3^\pm, \tag{26}$$

Pre-print version of the article: T. Kiefer, K. Graichen, and A. Kugi, “Trajectory tracking of a 3dof laboratory helicopter under input and state constraints”, *IEEE Transactions on Control Systems Technology*, vol. 18, pp. 944–952, 2010. DOI: 10.1109/TCST.2009.2028877
The content of this pre-print version is identical to the published paper but without the publisher’s final layout or copy editing.

see Fig. 6. Thereby, it is assumed that ψ_1^- and ψ_1^+ are asymptotic limits and $\psi_1(\xi_1, \psi_1^\pm)$ is strictly monotonically increasing, i.e. $\partial\psi_1/\partial\xi_1 > 0$. One possible choice of an appropriate saturation function is given by

$$\psi_1\left(\xi_1, \psi_1^\pm\right) = \psi_1^+ + \frac{\psi_1^- - \psi_1^+}{1 + \exp\left[m\,\xi_1\right]}. \tag{27}$$

The parameter m influences the slope at $\xi_1 = 0$ and is specified as $m = 4/(\psi_1^+ - \psi_1^-)$ which corresponds to the slope $\partial\psi_1/\partial\xi_1 = 1$ at $\xi_1 = 0$. The function (27) is depicted in Fig. 6.

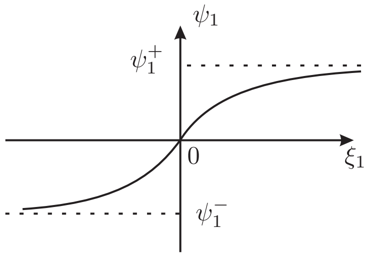

Fig. 6. Smooth saturation function $y_2^* = \psi_1(\xi_1, \psi_1^\pm)$ with the limits ψ_1^-, ψ_1^+ depending on the new state variable ξ_1.

In order to formulate the BVP in the new state variables, (25) has to be differentiated two times with respect to the time t. The first derivative is given by

$$\dot{y}_2^* = \frac{\partial\psi_1}{\partial\xi_1}\,\dot{\xi}_1, \tag{28}$$

whereby the state variable $\xi_2(t)$ is introduced in the form

$$\dot{\xi}_1 = \xi_2. \tag{29}$$

A further differentiation of (28) yields

$$\ddot{y}_2^* = \frac{\partial^2\psi_1}{(\partial\xi_1)^2}\,(\xi_2)^2 + \frac{\partial\psi_1}{\partial\xi_1}\,\dot{\xi}_2. \tag{30}$$

At this stage, the input constraints $v_2^- < v_2 < v_2^+$ according to (18) and (23) come into play. The consideration of these constraints is guaranteed by the use of a second saturation function

$$\dot{\xi}_2 = \psi_2(\tilde{v}_2, \psi_2^\pm) \tag{31}$$

depending on a new input $\tilde{v}_2$. Due to the assumption that $\partial\psi_1/\partial\xi_1 > 0$ the inequality $\ddot{y}_2^- \leq \ddot{y}_2^* \leq \ddot{y}_2^+$ can be rewritten by means of (30)

$$\frac{\tilde{\ddot{y}}_2^- - \frac{\partial^2\psi_1}{(\partial\xi_1)^2}\,(\xi_2)^2}{\frac{\partial\psi_1}{\partial\xi_1}} \leq \psi_2(\tilde{v}_2, \psi_2^\pm) \leq \frac{\tilde{\ddot{y}}_2^+ - \frac{\partial^2\psi_1}{(\partial\xi_1)^2}\,(\xi_2)^2}{\frac{\partial\psi_1}{\partial\xi_1}}, \tag{32}$$

where $\tilde{\ddot{y}}_2^\pm = \alpha_2(y_1^*, \psi_1(\xi_1, v_2^\pm))$ represent the substituted constraints (23). The left and right bounds in (32) directly determine the limits $\psi_2^\pm$ of the saturation function ψ_2

$$\psi_2^\pm = \psi_2^\pm\,(\xi_1, \xi_2) = \frac{\tilde{\ddot{y}}_2^\pm - \frac{\partial^2\psi_1}{(\partial\xi_1)^2}\,(\xi_2)^2}{\frac{\partial\psi_1}{\partial\xi_1}}. \tag{33}$$

Since no further differentiation of (30) is required, a $\mathcal{C}^0$ ramp–shaped function of the form

$$\psi_2\left(\tilde{v}_2, \psi_2^\pm\right) = \begin{cases} \psi_2^- & \text{if} \quad \tilde{v}_2 < \psi_2^- \\ \psi_2^+ & \text{if} \quad \tilde{v}_2 > \psi_2^+ \\ \tilde{v}_2 & \text{else} \end{cases} \tag{34}$$

Pre-print version of the article: T. Kiefer, K. Graichen, and A. Kugi, “Trajectory tracking of a 3dof laboratory helicopter under input and state constraints”, *IEEE Transactions on Control Systems Technology*, vol. 18, pp. 944–952, 2010. DOI: 10.1109/TCST.2009.2028877
The content of this pre-print version is identical to the published paper but without the publisher’s final layout or copy editing.

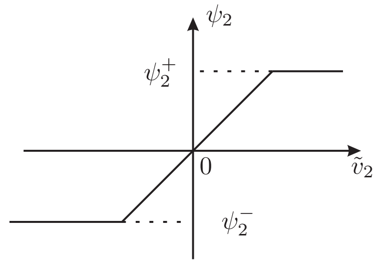

Fig. 7. Ramp–shaped saturation function $\psi_2\left(\tilde{v}_2, \psi_2^{\pm}\right)$ with the limits ψ_2^-, ψ_2^+ depending on the new input $\tilde{v}_2$.

suffices for all further calculations, see also Fig. 7.

The ODEs (29) and (31) form a dynamic system with the states ξ_1 and ξ_2 and the new input $\tilde{v}_2$. The output trajectory y_2^* and its time derivatives $\dot{y}_2^*$ and $\ddot{y}_2^*$ satisfying the constraints (24) and (21b) can be retraced algebraically from (25), (28), and (30).

In order to formulate the overall BVP for the helicopter subject to the input and state constraints, the BCs (12c) have to be transformed into the new coordinates ξ_1 and ξ_2. By inverting the saturation function (25)

$$\xi_1 = \psi_1^{-1}\left(y_2^*, \psi_1^{\pm}\right) \tag{35}$$

the BCs for the first state $\xi_1(t)$ for $t = 0, T$ are determined by $y_2^*(0) = q_{3,0}^* = 0$ and $y_2^*(T) = q_{3,T}^* = 0$. Inserting the homogeneous BCs $\dot{y}_2^*(0) = \dot{y}_2^*(T) = 0$ in (28) leads to $\dot{\xi}_1(0) = \dot{\xi}_1(T) = 0$ (with $\partial\psi_1/\partial\xi_1 > 0$). In view of (29), the boundary values for ξ_2 follow as

$$\xi_2(0) = 0, \quad \xi_2(T) = 0. \tag{36}$$

Since the input constraints (19) for v_1 do not directly influence the output constraints as it is the case for v_2, cf. (23), the input constraints (19) can be identically handled as in (31) by introducing a third ramp-shaped saturation function, see also Fig. 7,

$$\ddot{y}_1 = \psi_3(\tilde{v}_1, y_1^{\pm}) \tag{37}$$

depending on the new input $\tilde{v}_1$ and the limits $y_1^{\pm}$ according to (22). Thus summarizing the BVP (14a), (29), (31), (34), (36) and (37) leads to

$$\begin{aligned}
&\ddot{y}_1^* = \psi_3(\tilde{v}_1, y_1^{\pm}), && y_1^*(0) = q_{2,0}^*, && y_1^*(T) = q_{2,T}^*, && (38a)\\
& && \dot{y}_1^*(0) = 0, && \dot{y}_1^*(T) = 0, && \\
&\dot{\xi}_1 = \xi_2, && \xi_1(0) = 0, && \xi_1(T) = 0, && (38b)\\
&\dot{\xi}_2 = \psi_2(\tilde{v}_2, \psi_2^{\pm}), && \dot{\xi}_1(0) = 0, && \dot{\xi}_1(T) = 0, && \\
&\ddot{\eta}^* = \bar{\beta}(y_1^*, \ddot{y}_1^*, y_2^*), && \eta^*(0) = q_{1,0}^*, && \eta^*(T) = q_{1,T}^*, && (38c)\\
& && \dot{\eta}^*(0) = 0, && \dot{\eta}^*(T) = 0. &&
\end{aligned}$$

The solvability of the BVP (38) defined by 3 second–order ODEs and 12 BCs requires at least 6 free parameters. Therefore, the new inputs $\tilde{v}_1$ and $\tilde{v}_2$ are parametrized by means of ansatz functions $\tilde{v}_i = \Phi_i(t, p_i)$, $i = 1, 2$ with the sets of free parameters $p_i = (p_{i,1}, \ldots, p_{i,\kappa_i}), i = 1, 2$ where $\kappa_1 + \kappa_2 = 6$ holds. The numbers κ_i characterize the distribution of the 6 free parameters to the functions $\Phi_1(t, p_1)$ and $\Phi_2(t, p_2)$. A convenient choice for $\Phi_i(t, p_i)$ is given by the polynomials, see, e.g., [12], [14]

$$\Phi_i(t, p_i) = \sum_{k=1}^{\kappa_i} p_{i,k}\left(\left(\frac{t}{T}\right)^{k+1} - \frac{t}{T}\right), \quad i = 1, 2. \tag{39}$$

Pre-print version of the article: T. Kiefer, K. Graichen, and A. Kugi, “Trajectory tracking of a 3dof laboratory helicopter under input and state constraints”, *IEEE Transactions on Control Systems Technology*, vol. 18, pp. 944–952, 2010. DOI: 10.1109/TCST.2009.2028877
The content of this pre-print version is identical to the published paper but without the publisher’s final layout or copy editing.

It is obvious from (39) that the new input $\tilde{v}_i$ satisfies the homogeneous BCs $\tilde{v}_i(0) = \tilde{v}_i(T) = 0, i = 1, 2$. The BVP (38) is overdetermined by 12 BCs for 6 ODEs. Following the discussions in [10], the free parameter set $p_i = (p_{i,1}, \ldots, p_{i,\kappa_i})$ in the setup function $\Phi_i(t, p_i)$ must contain at least 2 elements to provide a sufficiently large number of free parameters for the solvability of the decoupled BVP, i.e. $\kappa_i \geq 2$, $i = 1, 2$. Following the discussion in Subsection III-B, the free parameters for the helicopter tracking maneuver are chosen as

$$\kappa_1 = 2, \quad \kappa_2 = 4 \tag{40}$$

in order to leave more "freedom" for the planning of the trajectory for the pitch angle $y_2^* = q_3^*$.

The solution of the BVP (38) with the boundaries (8) is again calculated using the bvp4c–algorithm of MATLAB now using the trajectories from Fig. 4 as initial guess[4]. Fig. 8 shows the resulting trajectories and the corresponding feedforward controls. It can be directly seen that the constraints in both the pitch angle q_3 as well as the constraints in the control inputs u_f and u_b are kept by the nominal trajectories. In order to comply with the constraints in $y_2^* = q_3^*$ the control input v_2^* has to be further increased during the rotation which results in an aggressive behavior of the control inputs v_1^*, v_2^* and u_f^*, u_b^*, respectively, which can especially be seen at $t = 5\mathrm{s}$ in Fig. 8.

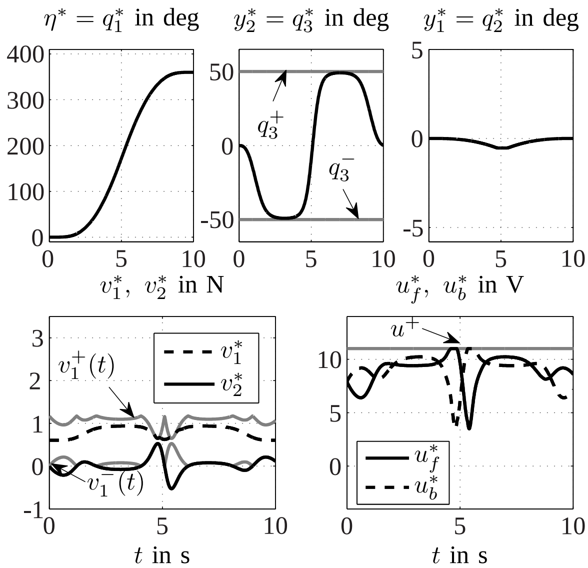

Fig. 8. Results of the feedforward control design taking into account input and output constraints.

Remark 2: Since both the output y_2^* and its second time derivative $\ddot{y}_2^*$ are constrained, special care has to be taken that no conflicts occur between the constraints (24) and (21b). If the output y_2^* approaches the constraints $y_2^* \to q_3^-$ or $y_2^* \to q_3^+$, the time derivatives (28) and (30) will approach zero, i.e. $\dot{y}_2^* \to 0$ and $\ddot{y}_2^* \to 0$. Hence, it must be guaranteed that the projected constraints (21b) for $\ddot{y}_2^*$ satisfy the inequality $\ddot{y}_2^- < 0 < \ddot{y}_2^+$ if $y_2^* \to q_3^-$ or $y_2^* \to q_3^+$ holds. In view of (21b) and (23), the inequality

$$a_3 \cos(y_1^*) \sin(y_2^*) + b_3 v_2^- < 0 < a_3 \cos(y_1^*) \sin(y_2^*) + b_3 v_2^+ \tag{41}$$

can be ensured by estimating conservative bounds for the input constraints v_2^- and v_2^+. With the parameters

[4]Note that the initial guess for the new states ξ_1 and ξ_2 in the new BVP (38) can be determined from the guess of y_2^* by means of (25), (28), respectively.

Pre-print version of the article: T. Kiefer, K. Graichen, and A. Kugi, "Trajectory tracking of a 3dof laboratory helicopter under input and state constraints", *IEEE Transactions on Control Systems Technology*, vol. 18, pp. 944–952, 2010. DOI: 10.1109/TCST.2009.2028877
The content of this pre-print version is identical to the published paper but without the publisher's final layout or copy editing.

$a_3 < 0$ and $b_3 > 0$, the above inequality can be written as

$$b_3 v_2^- < \underbrace{-a_3 \cos(y_1^*) \sin(y_2^*)}_{-|a_3| \leq 0 \leq |a_3|} < b_3 v_2^+ \,. \tag{42}$$

Hence, if the input constraints $v_2^\pm$ satisfy

$$v_2^- < -\frac{|a_3|}{b_3}, \quad v_2^+ > \frac{|a_3|}{b_3}, \tag{43}$$

the condition $\ddot{y}_2^- < 0 < \ddot{y}_2^+$ is ensured. With the helicopter parameters in Table I, this conservative estimation $v_2^- < -0.11\,\mathrm{N}$ and $v_2^+ > 0.11\,\mathrm{N}$ is satisfied by the actual constraints $v_2^\pm = \pm 0.58\,\mathrm{N}$ resulting from (18).

E. Feedback controller

As it was mentioned in Section II, the model (3) for the feedforward control design in Section III results from a simplification of the model. Thus it is necessary to design an additional closed–loop controller Σ^{FB}, cf. Fig. 3, to reject errors due to resulting model uncertainties and other disturbances. The controller under consideration is based on an optimal LQ–(linear quadratic) design. Since the reference feedforward trajectories $q_i^*,\ i = 1,2,3$, resulting from the solution of the BVPs (14) and (38), respectively, as well as the corresponding control inputs v_1^* and v_2^* are known the system (3) is linearized along these trajectories in order to derive a time–variant linear system. For this, the vectors

$$x = (q_1, \dot{q}_1, q_2, \dot{q}_2, q_3, \dot{q}_3)^T \text{ and } u = (v_1, v_2)^T \tag{44}$$

are introduced which are used to write the equations of motion according to (3) in the general form

$$\dot{x} = f(x,u). \tag{45}$$

Then, the linearized system reads as

$$\Delta\dot{x} = A(t)\,\Delta x + B(t)\,\Delta u \tag{46}$$

with

$$A(t) = \frac{\partial}{\partial x} f(x,u)\Big|_{x=x^*,u=u^*} \tag{47}$$

$$B(t) = \frac{\partial}{\partial u} f(x,u)\Big|_{x=x^*,u=u^*} \tag{48}$$

and $\Delta x = x - x^*$, $\Delta u = u - u^*$, $x^* = (q_1^*, \dot{q}_1^*, q_2^*, \dot{q}_2^*, q_3^*, \dot{q}_3^*)^T$, $u = (v_1^*, v_2^*)^T$.

The LQ–controller design is based on the minimization of the objective functional

$$I = \int_0^T \left(x^T Q x + u^T R u\right) \mathrm{d}t + x^T(T)\, M x(T) \tag{49}$$

with the positive semidefinite matrix $M \in \mathbb{R}^{6\times 6}$, the positive definite matrices $Q \in \mathbb{R}^{6\times 6}$, $R \in \mathbb{R}^{2\times 2}$ and the transition time T. The LQ–controller results from the solution of the Riccati–ODE, see, e.g., [22]

$$\begin{aligned} -\dot{P}(t) &= A(t)^T P(t) + P(t) A(t) + Q - \\ &\quad P(t) B(t) R^{-1} B(t)^T P(t) \\ P(T) &= M \end{aligned} \tag{50}$$

in the form

$$\Delta u = -K(t)\,\Delta x(t)\,,\ K(t) = R^{-1} B(t)^T P(t)\,, \tag{51}$$

where $K(t)$ is the time–variant feedback gain matrix.

Pre-print version of the article: T. Kiefer, K. Graichen, and A. Kugi, "Trajectory tracking of a 3dof laboratory helicopter under input and state constraints", *IEEE Transactions on Control Systems Technology*, vol. 18, pp. 944–952, 2010. DOI: 10.1109/TCST.2009.2028877
The content of this pre-print version is identical to the published paper but without the publisher's final layout or copy editing.

The time evolution of the entries of $K(t)$ for the given maneuver described in Section III-D are depicted in Fig. 9. Thereby, the two rows of the feedback gain matrix $K \in \mathbb{R}^{2\times 6}$ from (51) are plotted separately. In each case, the solid lines (–) refer to the components for $q_1, \dot{q}_1$, the dashed lines (- -) to those for $q_2, \dot{q}_2$ and the dotted lines ($\cdots$) to those for $q_3, \dot{q}_3$.

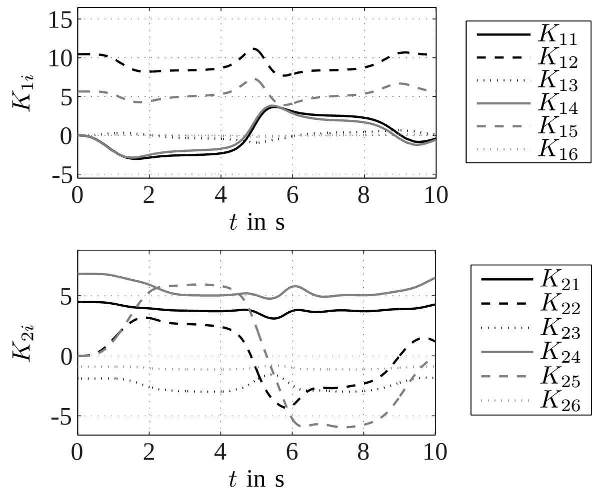

Fig. 9. $K_{1i}(t)$ (upper picture) and $K_{2i}(t)$, $i = 1, \ldots, 6$, (lower picture) of the LQ–controller (51) for the helicopter rotation with the transition time $T = 10\,\mathrm{s}$.

IV. Experimental results

The control scheme presented in Section III was implemented in the rapid prototyping system DSPACE with a sampling time $T_a = 1\mathrm{ms}$. The experimental results in form of the trajectories q_1, q_2 and q_3 can be seen in Fig. 10. Furthermore, Fig. 11 shows the required control inputs u_f and u_b. The nominal trajectories and control inputs are chosen according to Subsection III-D, see Fig. 8.

In Fig. 10 it can be seen that for the travel and the elevation angle, the measured trajectories q_1 and q_2 fit the nominal trajectories q_1^* and q_2^* in an excellent way. Only small deviations occur in the q_2–angle during the rotation. In the pitch angle q_3, the deviation is larger because of the intervention of the LQ–controller which is designed to hold the trajectories for the travel axis q_1 and the elevation axis q_2 near its desired pathes. Note that the trajectory of q_3 still remains within the constraints according to (7). In Fig. 11 the measured control inputs u_f and u_b are compared with the nominal ones. At the beginning and the end of the flight maneuver, it can be seen that the measured control input trajectory matches the nominal trajectory very well. As it becomes already apparent in the pitch angle q_3, especially after $t = 5s$, i.e. during the reversion of the pitch angle, the feedback controller has a large influence. This is due to the fact that the LQ–controller is optimized to keep the tracking error of the angles q_1 and q_2 at a minimum. Consequently, the constraints in the voltages u_f and u_b are not exactly met. Therefore, for the design of the feedforward controller, the constraints have to be chosen closer than the real constraints in order to provide reserves for the feedback controller.

Finally, it has to be stated that the main control task, namely the rotation about the travel axis q_1 in a finite time interval while keeping the input and state constraints, is very well performed. In addition, the LQ–controller design turns out to be very robust against model uncertainties and external disturbances. A presentation of the flight maneuver of the 3DOF helicopter laboratory experimental set–up can be found as an mpeg–video on the website http://www.acin.tuwien.ac.at/fileadmin/cds/videos/heli_ffwd.wmv.

Pre-print version of the article: T. Kiefer, K. Graichen, and A. Kugi, "Trajectory tracking of a 3dof laboratory helicopter under input and state constraints", *IEEE Transactions on Control Systems Technology*, vol. 18, pp. 944–952, 2010. DOI: 10.1109/TCST.2009.2028877
The content of this pre-print version is identical to the published paper but without the publisher's final layout or copy editing.

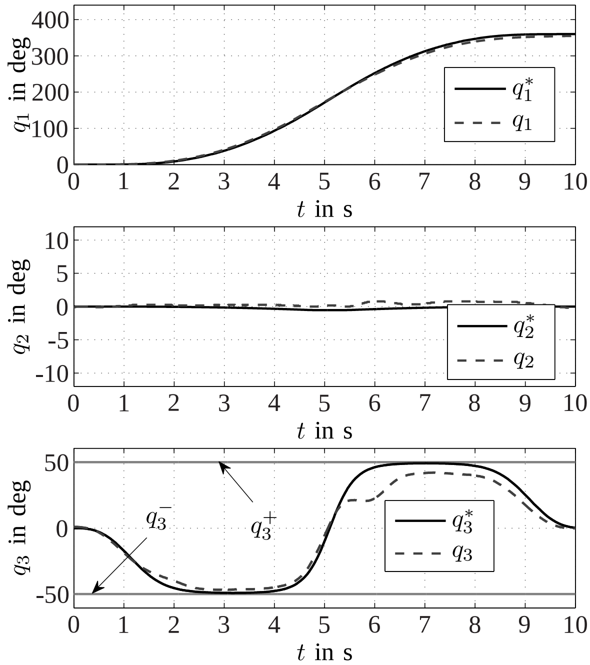

Fig. 10. Experimental results of the angles for constrained motion of the helicopter.

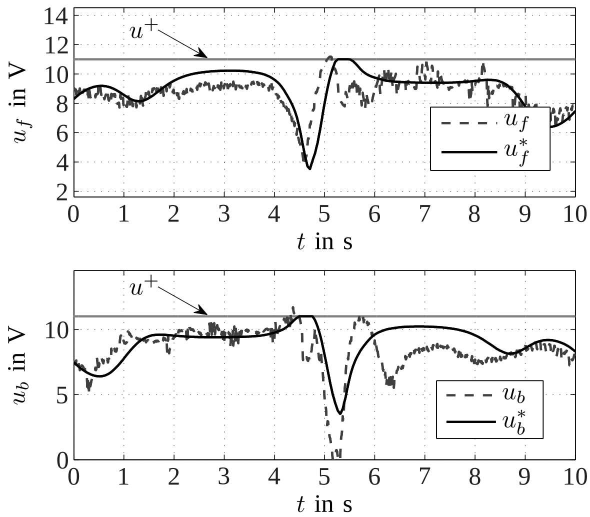

Fig. 11. Experimental results of the voltages for constrained motion of the helicopter.

V. Conclusion

This contribution is concerned with the systematic design of a tracking controller under input and state constraints for a laboratory helicopter realizing a prescribed flight maneuver. Since the laboratory helicopter has three mechanical degrees–of–freedom but only two control inputs it represents the important class of nonlinear underactuated mechanical systems. The control concept being proposed relies on a combination of a feedforward controller for trajectory tracking and a feedback controller to stabilize the trajectory error system. The feedforward control design treats the finite–time transition between two stationary points as a two–point BVP in the Byrnes–Isidori normal form of the system. This allows the systematic consideration

Pre-print version of the article: T. Kiefer, K. Graichen, and A. Kugi, "Trajectory tracking of a 3dof laboratory helicopter under input and state constraints", *IEEE Transactions on Control Systems Technology*, vol. 18, pp. 944–952, 2010. DOI: 10.1109/TCST.2009.2028877
The content of this pre-print version is identical to the published paper but without the publisher's final layout or copy editing.

of constraints in the inputs and outputs in order to achieve a fast trajectory tracking of the helicopter. The stabilizing feedback controller is designed as a time–variant LQ–controller which results from a linearization of the system along nominal trajectories. Experimental results prove the excellent tracking performance of the proposed feedforward/feedback control scheme.

REFERENCES

[1] *3DOF Helicopter system, product information*, Quanser Inc., Ontario, Canada, 2002, www.quanser.com.

[2] J. Apkarian, "Circuit cellar," *Internet Control*, vol. 110, 1999.

[3] X. Wei and P. Lautala, "Modeling and control design of a laboratory scale helicopter," in *CD–Proc. of the Conference on Applied Simulation and Modelling (ASM)*, Marbella, Spain, Mai 2003.

[4] A. Kutay, A. Calise, M. Idan, and N. Hovakimyan, "Experimental results on adaptive output feedback control using a laboratory model helicopter," *IEEE Transactions on Control Systems Technology*, vol. 13, no. 2, pp. 196–202, March 2005.

[5] D. Peaucelle, A. Fradkov, and B. Andrievsky, "Identification of angular motion model parameters for laas helicopter benchmark," in *Proc. IEEE International Conference on Control Applications*, Singapore, October 2007, pp. 825–830.

[6] B. Andrievsky, D. Peaucelle, and A. Fradkov, "Adaptive control of 3dof motion for laas helicopter benchmark: Design and experiments," in *Proc. the 2007 American Control Conference*, New York, July 2007, pp. 3312–3317.

[7] T. Kiefer, A. Kugi, and W. Kemmetmüller, "Modeling and flatness–based control of a 3 DOF helicopter laboratory experiment," in *Proc. of 6th IFAC–Symposium on Nonlinear Control Systems*, vol. 1, Stuttgart, Germany, 2004, pp. 207–212.

[8] M. Fliess, J. Lévine, P. Martin, and P. Rouchon, "Flatness and defect of non–linear systems: Introductory theory and examples," *Internat. Journal of Control*, vol. 61, pp. 1327–1361, 1995.

[9] M. Rathinam and R. Murray, "Configuration flatness of lagrangian systems underactuated by one control," *SIAM Journal of Control and Optimization*, vol. 36, no. 1, pp. 164–179, 1998.

[10] T. Kiefer, A. Kugi, K. Graichen, and M. Zeitz, "Feedforward and feedback tracking control of a 3 DOF helicopter experiment under input and state/output constraints," in *Proc. of 45th IEEE Conference on Decision and Control (CDC)*, San Diego, USA, 2006, pp. 1586–1593.

[11] K. Graichen, V. Hagenmeyer, and M. Zeitz, "A new approach to inversion-based feedforward control design for nonlinear systems," *Automatica*, vol. 41, pp. 2033–2041, 2005.

[12] K. Graichen and M. Zeitz, "Feedforward control design for nonlinear systems under input constraints," in *Control and Observer Design for Nonlinear Finite and Infinite Dimensional Systems*, ser. LNCIS 322, T. Meurer, K. Graichen, and E. Gilles, Eds. Springer, 2005, pp. 235–252.

[13] K. Graichen, "Feedforward control design for finite–time transition problems of nonlinear systems with input and output constraints," Ph.D. dissertation, Universität Stuttgart, http://elib.uni-stuttgart.de/opus/volltexte/2007/3004, November 2006.

[14] K. Graichen and M. Zeitz, "Feedforward control design for finite–time transition problems of nonlinear systems with input and output constraints," *IEEE Transactions on Automatic Control*, vol. 53, no. 5, pp. 1273–1278, 2008.

[15] R. Murray, Z. Li, and S. Sastry, *Robotic Manipulation*. Boca Raton: CRC Press, 1994.

[16] M. Spong and M. Vidyasagar, *Robot Dynamics and Control*, 1st ed. New York, USA: John Wiley & Sons, Inc., 1989.

[17] P. V. Kokotovic, J. O'Reilly, and H. K. Khalil, *Singular Perturbation Methods in Control: Analysis and Design*. Orlando, FL, USA: Academic Press, Inc., 1986.

[18] J. Seddon and S. Newman, *Basic Helicopter Aerodynamics*, 2nd ed. Oxford: Blackwell Science, 2002.

[19] S. Devasia, "Approximated stable inversion for nonlinear systems with nonhyperbolic internal dynamics," *IEEE Transactions on Automatic Control*, vol. 44, pp. 1419–1425, 1999.

[20] S. Devasia, D. Chen, and B. Paden, "Nonlinear inversion–based output tracking," *IEEE Transactions on Automatic Control*, vol. 41, pp. 930–942, 1996.

[21] K. Graichen and M. Zeitz, "Feedforward control design for nonlinear MIMO systems under input constraints," *International Journal of Control*, vol. 81, no. 3, pp. 417–427, 2008.

[22] P. Dorato, T. Chaouki, and C. Vito, *Linear Quadratic Control: An Introduction*. Malabar, Florida: Krieger Publishing Company, 2000.

Pre-print version of the article: T. Kiefer, K. Graichen, and A. Kugi, "Trajectory tracking of a 3dof laboratory helicopter under input and state constraints", *IEEE Transactions on Control Systems Technology*, vol. 18, pp. 944–952, 2010. DOI: 10.1109/TCST.2009.2028877
The content of this pre-print version is identical to the published paper but without the publisher's final layout or copy editing.